

## ILLITE FROM THE POTSDAM SANDSTONE OF NEW YORK: A PROBABLE NONCENTROSYMMETRIC MICA STRUCTURE

R. C. REYNOLDS JR.<sup>1</sup> AND C. H. THOMSON<sup>2</sup>

<sup>1</sup> Department of Earth Sciences, Dartmouth College, Hanover, New Hampshire 03755

<sup>2</sup> Department of Civil Engineering, University of Washington, Seattle, Washington 98195\*

**Abstract**—Illite from the Potsdam Sandstone (lower Ordovician) of Northwestern New York was studied by powder X-ray diffraction, scanning electron microscopy, and chemically analyzed and dated by the K/Ar method. The texture and ages of 360 and 392 Ma on two samples establish that the mineral is authigenic and relatively uncontaminated by Precambrian detritus. Random powder X-ray diffraction patterns show sharp and relatively intense 02/ and 11/ reflections, indicating an ordered structure. Comparisons with calculated patterns demonstrated that the mineral is not the common *1M* or *2M<sub>1</sub>* polytype. Instead, the experimental pattern is very similar to that of a *3T* polytype, but it agrees better with the calculated pattern of the octahedral *cis*-vacant, noncentrosymmetric (space group *C2*) structure found by Méring and Oberlin (1967) and Tsipursky and Drits (1984) in smectites, proposed for mica by Drits *et al.* (1984) and found by Zvyagin *et al.* (1985).

**Key Words**—Illite, Mica, Noncentrosymmetric, Polytype, Powder X-ray diffraction, Space group *C2*.

### INTRODUCTION

Studies of illite polytypism in soils and sedimentary rocks have focused on the *2M<sub>1</sub>*, *1M*, and *1Md* polytypes (e.g., Velde and Hower, 1963; Reynolds, 1963; Maxwell and Hower, 1967), although Levinson (1955) reported the *3T* polytype in decomposed granite. Środoń and Eberl (1984) reviewed this subject, and Austin *et al.* (1989) discussed the difficulties of identifying polytypes in sedimentary rocks and soils and demonstrated methods to enhance diagnostic X-ray reflections. Unfortunately, admixture of other clay minerals often makes it difficult or impossible, using powder X-ray diffraction (XRD) analysis, to detect and establish departures from the standard, well-known illite structures. Illites from some sandstones and most K-bentonites, however, are sufficiently pure so that excellent and highly revealing XRD patterns are easily obtained by long-count step-scan procedures.

Disordered dioctahedral micas commonly have space group *C2/m* (Bailey, 1984), but electron diffraction data lead Méring and Oberlin (1967) to conclude that the montmorillonite structure was noncentrosymmetric. The noncentric model placed montmorillonite in space group *C2* with the *M1* (*trans*) octahedral site occupied and one of the *M2* (*cis*) sites vacant.

The usual dioctahedral mica structure has a vacant *M1* site with both *M2* sites occupied, producing the mirror that characterizes space group *C2/m*. The *M1* site is larger, requiring the upper tetrahedral sheet in the centric 2:1 layer to shift relative to the lower one by more than the ideal value of  $a/3$ , leading to a typical monoclinic angle ( $\beta$ ) of about 101.3° (Bailey, 1984). The *cis*-vacant structure in *C2*, however, produces an

undershift with  $\beta = 99.13^\circ$  (Tsipursky and Drits, 1984; Drits *et al.*, 1984). An intermediate structure proposed by Drits *et al.* has each of the three octahedral positions  $\frac{2}{3}$  filled to produce a near ideal  $\beta$  value of 100.3°. Gavrilov and Tsipursky (1988) reported such a mineral from Jurassic sediments of the central Caucasus, and Zvyagin *et al.* (1985) described the hydrothermal occurrence of a dioctahedral *1M* mica with a structure very close to the ideal *cis*-vacant type.

Oblique-texture electron diffraction studies convinced Tsipursky and Drits (1984) that the Méring and Oberlin model was valid for some smectites. The former analyzed K-saturated smectites subjected to numerous wetting and drying cycles to minimize turbostratic stacking. The treated minerals produced the electron diffraction maxima necessary for a full structural determination, and they concluded that many montmorillonites contain significant proportions of *cis*-vacant layers. Drits *et al.* (1984) calculated three-dimensional XRD patterns of K-saturated montmorillonite that quantify the diagnostic 02/ : 11/ reflections for the *cis*-vacant model and its possible variations. Their results are applicable to illite, and we have based the present study on the seminal work of Tsipursky, Drits, and their co-workers.

S. Guggenheim (personal communication) pointed out to us that the *cis*- and *trans*-vacant structures are examples of cation ordering and that different polytype notations for them are unjustified. Therefore, in this paper we retain the usual mica polytype nomenclature prefixed by the labels *cv* (*cis*-vacant) or *tv* (*trans*-vacant) to identify the two. The designations *3T* and *2M<sub>1</sub>* are not prefixed because the *tv* layer is assumed for both.

## EXPERIMENTAL METHODS

*Sample description*

The sample studied was collected from an outcrop approximately 2.5 miles northeast of the town of Alexandria Bay, New York. This site (Carl and Van Diver, 1971) exposes the basal Potsdam unconformity and the Precambrian basement. Previous work by Cupery and Selleck (1987) described well-crystallized illite within the basal Potsdam, and scanning electron microscope (SEM) examination suggested that the illite is authigenic (Selleck, personal communication, 1989). Nine samples were taken from just above the Cambrian-Precambrian unconformity. All contain illite, but the sample reported herein contains the highest concentration.

The rock in hand-specimen is a pale tan (nearly white), friable, medium-grained sandstone with pink streaks defining cross-beds. Thin-section studies showed very well-sorted and well-rounded to subangular quartz grains with optically continuous quartz overgrowths. The rock consists of almost pure quartz. Illite is present as a barely resolvable felted matrix that fills sparse pores provided by the overgrowth fabric. SEM images of the illite show flame-like crystals, rooted on quartz grains, that extend into the pores to produce a texture typical of authigenic growth. This description is consistent with those provided by Selleck (personal communication, 1989), who noted similar textures throughout the Potsdam Sandstone for kaolinite, chlorite, and illite.

*Age determination*

K/Ar age determinations were made on separated <2  $\mu\text{m}$  powders from two samples higher in the outcrop than the sample described here. The measurements were made by Krueger Enterprises Inc., Geochron Laboratories Division, Cambridge, Massachusetts. The samples yielded K/Ar dates of  $360 \pm 9$  Ma and  $392 \pm 9$  Ma, which are comparable to unpublished K/Ar dates ( $355 \pm 12$  Ma) by Selleck (personal communication, 1989) on illite from the Potsdam Sandstone in the Alexandria Bay region. The sample selected for detailed study contains small amounts of  $1M$  and  $2M_1$  mica, an estimated 6% and 10% respectively, but the measured ages are about 100 My younger than the deposition age (early Ordovician), establishing the dominant mineral as authigenic and relatively uncontaminated by Precambrian detritus.

*Chemical analysis*

Bulk chemical analysis consisted of X-ray fluorescence on a portion of a <2  $\mu\text{m}$  separate by X-ray Assay Laboratories, Don Mills, Ontario, and D. Lange measured F by electron microprobe. Total Fe was calculated as  $\text{Fe}_2\text{O}_3$ . The analysis and the resulting formula are given in Table 1. The analysis is similar to that for

Table 1. Chemical analysis and formula of the Potsdam illite.

	Raw data	Corrected <sup>1</sup>	Per 11 oxygens	Cations
$\text{SiO}_2$	52.1	51.26	54.58	3.396
$\text{Al}_2\text{O}_3$	28.7	29.27	31.16	2.285
CaO	0.15	0.15	0.16	0.011
MgO	1.93	1.98	2.11	0.196
$\text{Na}_2\text{O}$	0.16	0.16	0.17	0.021
$\text{K}_2\text{O}$	7.95	8.19	8.72	0.692
$\text{Fe}_2\text{O}_3$	2.80 <sup>2</sup>	2.88	3.07	0.144
MnO	0.01	0.01	0.01	—
$\text{TiO}_2$	0.024	0.024	0.03	0.001
F	0.31	0.31	0.07	
LOI	6.0	6.07		
Total	100.13			

<sup>1</sup> Corrected for 2% quartz and 0.7% kaolinite.

<sup>2</sup> Total Fe calculated as  $\text{Fe}^{3+}$ .  $\text{K}_{0.69}\text{Na}_{0.02}\text{Ca}_{0.01}(\text{Al}_{1.68}\text{Fe}_{0.14}\text{Mg}_{0.20})(\text{Si}_{3.40}\text{Al}_{0.60})\text{O}_{10}(\text{OH}_{1.93}\text{F}_{0.07})$

an average illite, as reported by Weaver and Pollard (1973), and the F content is not exceptional for micas. The abnormally high loss on ignition might indicate the presence of water molecules in some interlayer positions.

*Sample preparation*

Matrix clay was separated by light crushing, mixing about 25 g of the crushed rock with 150 ml of water in a 300 ml plastic bottle, and agitating for 2 hr in an automatic sample shaker. The sandstone was so friable that it quickly broke down into almost sand-sized aggregates. The <2  $\mu\text{m}$  fraction (e.s.d.) was isolated by centrifugation after dispersion in 0.001 M sodium pyrophosphate. The clay fraction was freeze-dried, and a randomly oriented sample was prepared by the side-loading procedure using a sample holder 3 cm long, 2.35 cm wide, and 0.15 cm deep. A 200 mg aliquot of the freeze-dried powder was redispersed in 2 ml of water, completely pipetted onto a glass slide, and dried at 80°C. It was analyzed air-dried and after vapor solvation with ethylene glycol at 60°C for 12 hr.

*X-ray diffraction*

Data were collected with a Siemens D-500 X-ray diffractometer equipped with a Cu anode tube and a diffracted beam graphite monochromator. Experimental conditions involved 1° divergence and 0.15° receiving slits, a diffracted-beam Soller slit (2°), and tube operating conditions of 40 mA-40 kV. The instrument produced 15,000 counts per second at the top of the 101 quartz peak recorded from a standard quartz powder. Goniometer alignment was checked by reference to the XRD pattern of the quartz calibration standard between 20 and 65°  $2\theta$ . Accuracy was within  $\pm 0.01^\circ 2\theta$ .

The diffraction pattern of the random-powder illite preparation was recorded by the step-scan method,

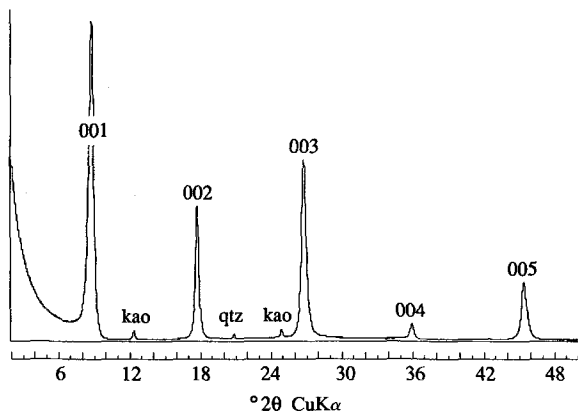


Figure 1. Potsdam illite, air-dried  $<2 \mu\text{m}$  oriented aggregate.

using 20 s count times at increments of  $0.02^\circ 2\theta$ . Data for the air-dried and ethylene glycol solvated oriented aggregates were obtained using a  $0.02^\circ$  step size and a 10 s/step count time.

#### Computer modeling

Random powder XRD patterns were calculated by a refined version of the methods described by Reynolds (1989a, 1989b). Calculated  $3T$ ,  $2M_1$ , and  $tv-1M$  diffraction patterns are based on the  $T$  layer of Drits *et al.* (1984), with  $a = 5.199 \text{ \AA}$ ,  $b = 9.005 \text{ \AA}$ ,  $c = 10.164 \text{ \AA}$ , and  $\beta = 101.3^\circ$ . The  $cv-1M$  calculations used the atomic coordinates of the  $C$  layer of Drits *et al.* with  $a = 5.199 \text{ \AA}$ ,  $b = 9.005 \text{ \AA}$ ,  $c = 10.09 \text{ \AA}$ , and  $\beta = 99.13^\circ$ . The latter assumed a random interstratification of equal proportions of the two possible  $cv$  enantiomorphs. All calculated diffraction patterns apply to crystals made up of 60 unit cells along  $X$ , 30 unit cells along  $Y$ , and a defect-free distance of 12 unit cells along  $Z$ , with maximum  $Z = 32$  unit cells.  $2M_1$  and  $3T$  calculations did not use unit cells as commonly defined for these structures. Instead,  $10\text{-\AA}$  layers were stacked in appropriate fashions along  $Z$ , and the interlayer phase effects and the appropriate structure factors for rotated 2:1 layers were applied.

Atomic scattering factors were calculated (Wright, 1973) for half-ionized O, Si, and Al and for fully ionized  $\text{Fe}^{2+}$  (corrected for dispersion) and K. Isotropic atomic thermal vibration parameters ( $b$ ) of 2 and 1.5 were used for anions and cations respectively.

## RESULTS

### 001 reflections and one-dimensional character

The diffraction pattern of the air-dried, oriented aggregate is typical of a nearly pure illite except for an estimated 0.7% kaolinite and 2% quartz (Figure 1). Small changes in line breadth occurred upon ethylene glycol solvation, indicating that the illite is slightly expandable—perhaps by 2%. Percent quartz was esti-

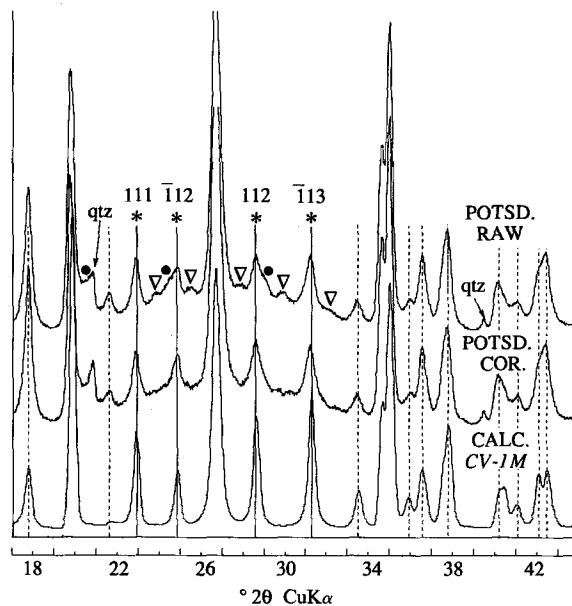


Figure 2. Top trace is the uncorrected random power XRD pattern ( $<2 \mu\text{m}$ ) for the Potsdam illite. Middle trace is the corrected pattern from which calculated  $tv-1M$  and  $2M_1$  patterns have been subtracted. Bottom trace is a calculated pattern for the  $cv-1M$  structure.

mated by comparing the absolute intensity of the 112 quartz peak with that of the same reflection from a pure quartz powder (corrected for the difference in mass absorption coefficients), and kaolinite was determined by comparing the intensities of the kaolinite 002 and illite 003 from the oriented aggregate with those calculated by NEWMOD (Reynolds, 1985).

### Three-dimensional structure

The random powder pattern for the raw data is shown by Figure 2. Preferred orientation is indicated by the relatively high intensity ratio of the 002/(020;110) reflections at  $17.75$  and  $19.9^\circ 2\theta$  respectively, but the quality of the data is sufficient to show many three-dimensional peaks. Solid dots mark the positions of strong  $k \neq 3n$   $tv-1M$  lines, and triangles depict the strongest  $k \neq 3n$   $2M_1$  reflections. Calculated diffraction patterns for  $tv-1M$  and  $2M_1$  polytypes were subtracted by trial-and-error from the experimental pattern to produce the corrected result of Figure 2. The integrated intensities of the diffraction patterns were measured over the unresolved  $20l$ ;  $13l$  peaks between  $34^\circ$  and  $36^\circ 2\theta$ . These intensities were used to adjust the experimental and calculated patterns to a common intensity base so that quantitative estimates could be made of the two quantities subtracted.

The lowermost trace on Figure 2 is a calculated pattern for a  $cv-1M$  structure, and the approximate correspondence between it and the Potsdam illite is evident. The solid and starred vertical lines identify the

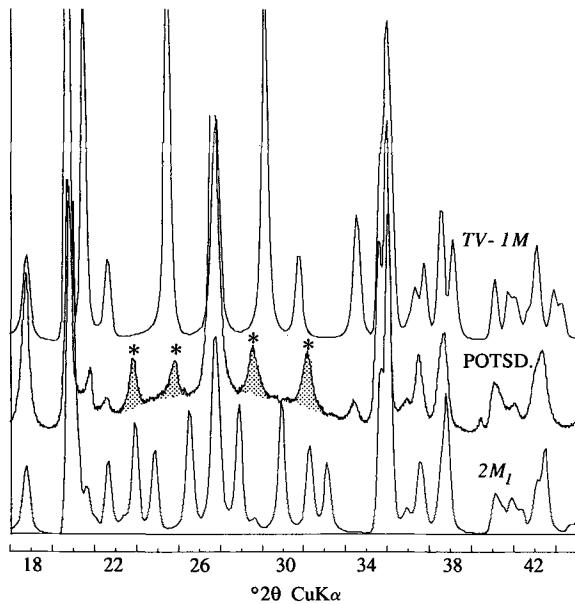


Figure 3. Comparisons among calculated powder patterns for the *tv-1M* and *2M<sub>1</sub>* structures and the corrected experimental pattern for the Potsdam illite. Shaded peaks on the Potsdam pattern are the *11l* reflections that are diagnostic for the *cv-1M* or *3T* structures.

*11l* reflections that are diagnostic for the *cv-1M* and *3T* structures. These four peaks, roughly of equal intensity, demonstrate that the Potsdam illite is certainly not a *2M<sub>1</sub>* or *tv-1M* polytype (see Figure 3). Their relative intensities are characteristic of a *cv-1M* or *3T* structure, but differentiation between the latter two is difficult, and Thomson previously (1990) identified the Potsdam illite as a *3T* polytype.

Figure 4 shows a comparison between powder patterns calculated for *cv-1M* and *3T* polytypes. The patterns are remarkably similar, with *d* significantly different for only a few reflections (see Table 3). The  $2\theta$  range outlined on Figure 4 and shown in more detail by Figure 5 is diagnostic. Neither calculated pattern perfectly reproduces the experimental trace in Figure 5, but the *cv-1M* pattern is closest to the experimental results.

Measured *d* values and integrated intensities (Table 2) were read from experimental and calculated patterns that were plotted to greatly expanded horizontal and vertical scales. Quartz 102 and 211 reflections were treated as an internal standard and corresponding adjustments were made to the  $2\theta$  scale on the experimental pattern.

The first 10 intensity entries in Table 2 yielded  $R = 0.14$  according to

$$R = \frac{|F_o - nF_c|}{\sum F_o},$$

where *F* is the square root of the intensity divided by

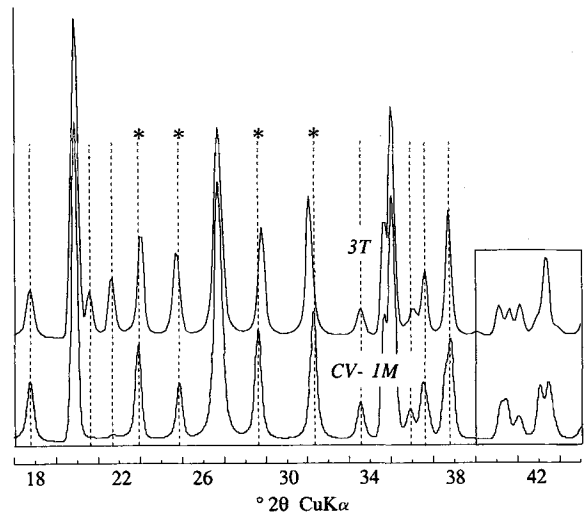


Figure 4. Calculated powder patterns for the *3T* and *cv-1M* structures.

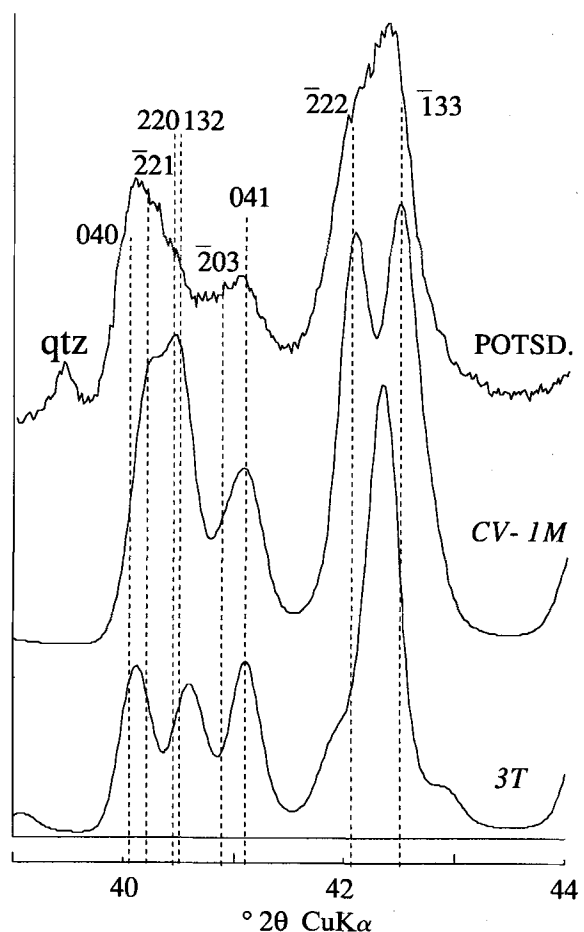


Figure 5. Detail of the area indicated in Figure 4. The top trace is the experimental pattern, the center is the calculated *cv-1M* profile, and the bottom shows the calculated *3T* pattern.

Table 2. Comparisons between observed and calculated  $d$  and intensity.

$hkl$	$d(\text{obs.})^1$	$d(\text{calc.})^2$	$I(\text{obs.})$	$I(\text{calc.})^2$
020, 110	4.48	4.47	100	100
021	4.11	4.09	5.2	1.4
111	3.882	3.878	21.9	33.6
$\bar{1}12$	3.579	3.579	14.7	18.5
112	3.118	3.116	31.6	39.9
$\bar{1}13$	2.864	2.859	37.7	52.0
023	2.680	2.672	7.1	13.2
$\bar{2}01, 130$	2.589	2.588		
200, $\bar{1}31$	2.564	2.561	173.0	119.9
$\bar{2}02, 131$	2.458	2.459	32.2	25.7
201, $\bar{1}32$	2.383	2.379	53.9	49.5
$\bar{2}03, 041$	2.197	2.197		
005	1.996	1.994		
060, $\bar{2}06, \bar{3}14$	1.501	1.503		

<sup>1</sup>  $2\theta$  scale adjusted to quartz reflections.

<sup>2</sup> Based on the  $cv$ - $1M$  structure of Drits *et al.* (1984).

the random powder Lorentz-polarization factor and  $n$  is a normalization constant given by

$$n = \frac{\sum F_o}{\sum F_c}$$

The significance of  $R$  is reduced by the use of only 10 reflections; in addition,  $R$  is a poor discriminator between the  $cv$ - $1M$  and  $3T$  structures if only these ten reflections are used in its computation.

$1M$  and  $3T$  structures were tested for compatibility with experimental  $d$ -spacings. For the hexagonal option,  $c$  was set equal to  $3.5 \cdot d(005)$  (Table 2), and  $a$  was computed for each of the five single peaks (see Table 3). Mean  $a$  was then used to compute  $d$  for each, and the root-mean-square difference (RMSD) between these and the experimental  $d$ -values was calculated. The relatively large ( $\pm 0.05 \text{ \AA}$ ) standard deviation of  $a$  about mean  $a$  suggests incompatibility of the experimental data with a hexagonal structure.

Parameters for a  $1M$  structure were obtained from the simultaneous solution of two expressions to give  $a$ ,  $c$ , and  $\beta$  (Sakharov *et al.* 1990).

$$\frac{1}{d^2(112)} = \frac{1}{(a \sin \beta)^2} + \frac{1}{b^2} + \frac{4}{(c \sin \beta)^2} - \frac{4 \cos \beta}{a \sin \beta c \sin \beta}$$

$$\frac{1}{d^2(\bar{1}12)} = \frac{1}{(a \sin \beta)^2} + \frac{1}{b^2} + \frac{4}{(c \sin \beta)^2} + \frac{4 \cos \beta}{a \sin \beta c \sin \beta}$$

$b$  was assumed to be equal to  $6 \cdot d(060)$ , despite possible interferences from other reflections, and  $c \sin \beta = 5 \cdot d(005)$ . Comparison of this model with the  $cv$ - $1M$  unit cell parameters of Drits *et al.* (1984) is shown by Table 3.

Table 3. Comparisons between experimental  $d$  and values calculated for monoclinic and hexagonal unit cells.

$1M^1$			$3T^2$	
$hkl$	$d(\text{calc.})$	$d(\text{obs.})$	$hkl$	$d(\text{calc.})$
021	4.105	4.11	103	4.107
111	3.876	3.882	104	3.861
$\bar{1}12$	3.579	3.579	105	3.601
112	3.118	3.118	107	3.012
$\bar{1}13$	2.862	2.864	108	2.879
023	2.676	2.680	109	2.676
$1M$ Unit Cell <sup>1</sup>			Hexagonal Unit Cell <sup>2</sup>	
$a = 5.197, b = 9.006$			$a = 5.204 \pm 0.05 \text{ \AA}$	
$c = 10.108(4) \text{ \AA}$			$c = 29.940 \text{ \AA}$	
$\beta = 99.13^\circ$				
R.M.S. calc. - obs.			R.M.S. calc. - obs.	
$= 0.0037 \text{ \AA}$			$= 0.0154 \text{ \AA}$	
$cv$ - $1M$ : Drits <i>et al.</i> (1984)				
$a = 5.199, b = 9.005$				
$c = 10.09 \text{ \AA}$				
$\beta = 99.13^\circ$				

## DISCUSSION

Figure 3 demonstrates that the Potsdam illite is not a  $tv$ - $1M$  or  $2M_1$  polytype. Calculated patterns, not shown here, for  $20$  and  $2M_2$  polytypes are equally unrealistic, leaving  $3T$  or  $cv$ - $1M$  structures as the likely possibilities.

The experimental XRD pattern resembles the calculated  $cv$ - $1M$  pattern over the  $2\theta$  range  $39$  to  $44^\circ$  (Figure 5), although the  $040$  peak on the experimental profile is too weak and resolution of the  $\bar{2}22$  and  $\bar{1}33$  reflections is poorly matched between calculated and observed patterns. The calculated  $3T$  pattern, on the other hand, agrees poorly with the data between  $39^\circ$  and  $44^\circ$  and produces an unrealistic single peak instead of a double peak between  $42^\circ$  and  $43^\circ 2\theta$ .

The  $d$ -values provide a more definitive analysis. Table 3 shows that spacings for the six single reflections corresponding to the  $02l; 11l$  ( $l > 0$ )  $1M$  indices are inconsistent with an hexagonal structure. The standard deviation of calculated  $a$  about mean  $a$  ( $\pm 0.05 \text{ \AA}$ ) is more than ten times the estimated experimental error for measurements in this  $2\theta$  interval. In addition, the RMSD between observed and calculated spacings based on mean  $a$  is roughly four times as large as the same statistic for the model  $1M$  structure.

The quality of diffraction data shown by Figure 2 limits the accuracy of  $d$  to about  $\pm 0.003$  to  $\pm 0.002 \text{ \AA}$  over the range  $20^\circ$  to  $34^\circ 2\theta$ . The RMSD between model  $1M$  and observed  $d$ -values is  $\pm 0.0037 \text{ \AA}$ , although two of the six observed spacings were used to parameterize the  $1M$  structure and thus have zero error by definition. Nevertheless, this RMSD is near the experimental error in contrast to the value for the  $3T$  spacings, which is about four times as large.

Twinned *1M* and *3T* structures give similar diffraction patterns (see Güven and Burnham, 1967). Sadanaga and Takéuchi (1961) have pointed out, however, that if  $b = a\sqrt{3}$ , a twinned *1M* crystal produces *d*-values that correspond to a hexagonal unit cell for which *a* is equal to *a* for the *1M* unit cell. The *d*-values from the experimental pattern, however, are inconsistent with an hexagonal cell, thus eliminating this twinned *1M* possibility. The illite could be a twinned non-orthorhombic *1M* structure, but the data fit so well a *1M* model with  $b = a\sqrt{3}$  that the latter argument is unlikely because it depends too heavily on coincidence. We conclude that the Potsdam illite is a *1M* polytype, based on 1) the poor agreement between model *3T* and observed *d*-values, 2) the better agreement between calculated *1M* and observed *d*-values, 3) the large standard deviation of calculated *a* about mean *a* for an hexagonal model, and 4) supporting evidence given by the diffraction patterns of Figure 5.

Two kinds of evidence suggest that the Potsdam illite is a *cv* layer type. The first is the cell geometry. Drits *et al.* (1984) maintained that  $c \cos \beta/a > -0.383$  indicates some occupancy of the *M1* octahedral site, and that each of the three octahedral sites are  $\frac{2}{3}$  filled if  $c \cos \beta/a = -\frac{1}{3}$ .  $c \cos \beta/a$  is further increased if the *M1* site is more than  $\frac{2}{3}$  filled, with the limit of  $-0.308$  for a *cv* structure (one vacant *M2* site). The *1M* unit cell deduced from experimental data (Table 3) has  $\beta = 99.13^\circ$  and  $c \cos \beta/a = -0.310$ , which is very close to the *cv* limit of  $-0.308$ , providing strong evidence for such a structure.

Other evidence for the *cv* structure lies in the intensities of the diagnostic 02:11 reflections. Figure 2 shows that these and other reflections show generally good agreement between observed intensities and those calculated for the *cv* structure of Drits *et al.* (1984), i.e.,  $c \cos \beta/a = -0.308$ .  $R = 0.14$ , based on 10 peaks, suggests that the structure is essentially correct but requires refinement of atomic coordinates (Buerger, 1960).

Drits *et al.* derived the atomic coordinates used herein by transformation of a *tv* to a *cv* unit cell; they did not refine a real *cv* structure. Their coordinates are idealized and may not be entirely applicable here; alternatively, the illite may have somewhat less than full occupancy of the *M1* site (suggested by V. A. Drits, personal communication, 1992). Regardless of changes that might be achieved by refinements beyond the scope of this study, the XRD data for the illite, in our opinion, can be best reconciled with a *cv-1M* structure or one with very similar cation ordering.

*cv-1M* and *3T* polytypes can be distinguished by an analysis of *d*-values if the crystallites are large and ordered. The diagnostic reflections have indices of the type  $k \neq 3n$ , and they are broadened by rotational stacking disorder ( $n.60^\circ$  or  $n.120^\circ$ ). Small crystallite size broadens all, and the result of either or both of these conditions could be such a loss of definition that *cv-*

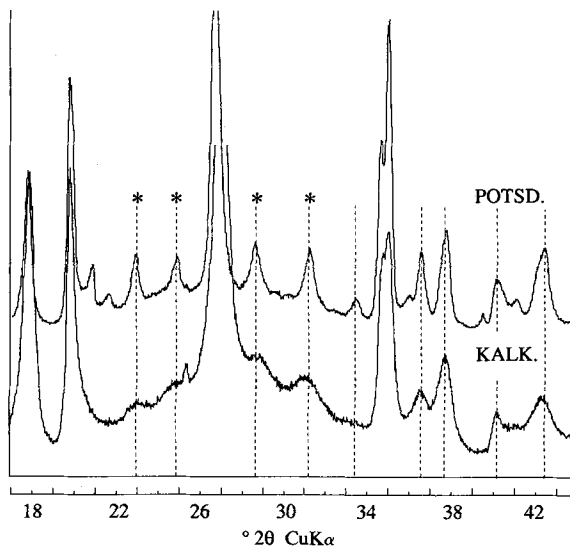


Figure 6. Comparison between diffraction patterns of the Potsdam illite and the heated ( $<1 \mu\text{m}$ ;  $350^\circ\text{C}$ ) Kalkberg K-bentonite.

*1M* and *3T* structures are no longer differentiable. Even for samples that produce sharp reflections, it might not be possible to detect admixture of small amounts of either with large amounts of the other.

Figure 6 compares the Potsdam illite with the Devonian Kalkberg K-bentonite (Reynolds and Hower, 1970) after heating to  $350^\circ\text{C}$ . The two patterns are similar, although the broad 20:13 reflections for the Kalkberg sample indicate particle-size broadening, and the 02:11 peaks are additionally broadened by  $n.120^\circ$  rotational stacking disorder ( $n.60^\circ$  disorder is minimal, based on 20:13 peak resolution, which is diminished by this type of disorder; see Sakharov *et al.*, 1990). Patterns similar to those in Figure 6 have been reported by Reynolds (1992) for K-bentonites from the overthrust belt of Montana, though they were identified as *3T* or twinned *tv-1M* polytypes; and diffraction patterns like that of the Potsdam illite have been noted for illites from the Rotliegendes (North Sea Basin) and Mount Simon (Illinois Basin) sandstones (Mingchou Lee, personal communication, 1992).

## CONCLUSIONS

Previous reports of noncentric dioctahedral 2:1 phyllosilicates in sedimentary rocks have dealt with the smectite minerals; and, to our knowledge, there is no published, documented example of a *cv* dioctahedral illite in sedimentary rocks, though Zvyagin *et al.* (1985) report it in hydrothermal associations. We conclude that illite from the Potsdam Sandstone of New York has the *cv 1M* structure proposed by Drits *et al.* (1984) and suggest that this type of cation ordering and its rotationally disordered variants may be common enough to warrant the attention of clay mineralogists.

The dioctahedral *cv-IM* structure is easily distinguished by XRD from the dioctahedral  $2M_1$  and *tv-IM* polytypes. It may be impossible by X-ray analysis alone to differentiate the *cv-IM* from the  $3T$  polytype if crystallite size is small enough to cause significant line-broadening and/or if the crystallites are rotationally disordered.

$R = 0.14$  indicates that the *cv-IM* atomic coordinates need refinement. In addition, a structure should be considered that has somewhat less than full occupancy of the  $M1$  site. Among other models not considered here is admixture of *cv-IM* crystals with a highly disordered (*IMd*) component composed of *cv* or *tv* layers.

#### ACKNOWLEDGMENTS

Grateful acknowledgment is made to the American Chemical Society for funding substantial portions of this work by means of Grant 23613-AC2. In addition, we thank the Mobil Foundation and the Chevron Oil Field Research Company for support that has made it possible for Dartmouth College to keep pace with new developments in X-ray diffraction technology.

#### REFERENCES

- Austin, G. S., Glass, H. D., and Hughes, R. E. (1989) Resolution of the polytype structure of some illitic clay minerals that appear to be  $1M_d$ : *Clays & Clay Minerals* **37**, 128–134.
- Bailey, S. W. (1984) Crystal chemistry of the true micas: in *Micas*, S. W. Bailey, ed., Mineralogical Society of America, Reviews in Mineralogy **13**, 13–60.
- Buerger, M. J. (1960) *Crystal-Structure Analysis*: John Wiley and Sons, New York.
- Carl, J. D. and Van Diver, B. B. (1971) Some aspects of Grenville geology and the Precambrian/Paleozoic unconformity, Northwest Adirondacks, New York: *Field Trip Guidebook, N.Y.S.G.A., 43rd Annual Meet.*, A1–A39.
- Cupery, S. and Selleck, B. (1987) Diagenesis and clay mineralogy of the Potsdam Sandstone in Northwestern New York: *Prog. Abst., Geol. Soc. Amer., Northeastern Section Meeting* **19**(1), 10.
- Drits, V. A., Plançon, B. A., Sakharov, B. A., Besson, G., Tshipursky, S. I., and Tchoubar, C. (1984) Diffraction effects calculated for structural models of K-saturated montmorillonite containing different types of defects: *Clay Miner.* **19**, 541–561.
- Gavrilov, Y. O. and Tshipursky, S. I. (1988) Clay minerals of lower and middle Jurassic sediments of structural and facies zones of the central Caucasus: *Lithology and Mineral Resources, Consultants Bureau, New York* **22**, 570–582.
- Güven, N. and Burnham, C. W. (1967) The crystal structure of  $3T$  muscovite: *Zeit. Kristallogr. Kristallgeom.* **125**, 163–183.
- Levinson, A. A. (1955) Studies in the mica group: Polymorphism among illites and hydrous micas: *Amer. Mineral.* **40**, 41–49.
- Maxwell, D. T. and Hower, J. (1967) High-grade diagenesis and low grade metamorphism of illite in the Precambrian Belt series: *Amer. Mineral.* **52**, 843–857.
- Méring, J. and Oberlin, A. (1967) Electron-optical study of smectites: *Clays & Clay Minerals*, 17th Nat. Conf., Pergamon Press, 3–25.
- Reynolds, R. C. (1963) Potassium-rubidium ratios and polymorphism in illites and microclines from the clay size fraction of Proterozoic carbonate rocks: *Geochem. et Cosmochim. Acta* **27**, 1097–1112.
- Reynolds, R. C. (1985) *NEWMOD, a Computer Program for the Calculation of Basal X-Ray Diffraction Intensities of Mixed-Layered Clays*, R. C. Reynolds, Hanover, New Hampshire.
- Reynolds, R. C. (1989a) Principles of powder diffraction: in *Modern Powder Diffraction*, D. L. Bish and J. E. Post eds., Mineralogical Society of America, Reviews in Mineralogy **20**, 1–17.
- Reynolds, R. C. (1989b) Diffraction by small and disordered crystals: in *Modern Powder Diffraction*, D. L. Bish and J. E. Post eds., Mineralogical Society of America, Reviews in Mineralogy **20**, 145–181.
- Reynolds, R. C. (1992) X-ray diffraction studies of illite/smectite from rocks,  $<1 \mu\text{m}$  randomly oriented powders, and  $<1 \mu\text{m}$  oriented powder aggregates: The absence of laboratory-induced artifacts: *Clays & Clay Minerals* **40**, 387–398.
- Reynolds, R. C. and Hower, J. (1970) The nature of interlayering in mixed-layer illite-montmorillonites: *Clays & Clay Minerals* **18**, 25–36.
- Sadanaga, R. and Takéuchi, Y. (1961) Polysynthetic twinning of micas: *Zeit. Kristallogr.* **116**, 406–429.
- Sakharov, B. A., Besson, G., Drits, V. A., Kamenava, M. Y., Salyn, A. L., and Smoliar, B. B. (1990) X-ray study of the nature of stacking faults in the structure of glauconites: *Clay Miner.* **25**, 419–435.
- Środoń, J. and Eberl, D. D. (1984) Illite: in *Micas*, S. W. Bailey, ed., Mineralogical Society of America, Reviews in Mineralogy **13**, 495–544.
- Thomson, C. H. (1990) *Authigenic 3T illite in the Potsdam Sandstone, New York*: M.S. dissertation, Dartmouth College, Hanover, New Hampshire, 60 pp.
- Tshipursky, S. I. and Drits, V. A. (1984) The distribution of octahedral cations in the 2:1 layers of dioctahedral smectites studied by oblique-texture electron diffraction: *Clay Miner.* **19**, 177–193.
- Velde, B. and Hower, J. (1963) Petrological significance of illite polymorphism in Paleozoic sedimentary rocks: *Amer. Mineral.* **48**, 1239–1254.
- Weaver, C. E. and Pollard, L. D. (1973) *The Chemistry of Clay Minerals: Developments in Sedimentology* **15**, Elsevier.
- Wright, A. C. (1973) A compact representation for atomic scattering factors: *Clays & Clay Minerals* **21**, 489–490.
- Zvyagin, B. B., Robotnov, V. T., Sidorenko, O. V., and Kotelnikov, D. D. (1985) Unique mica with noncentrosymmetric layers: *Izvestiya Akad. Nauk SSSR, Geol.* **35**, 121–124 (in Russian).

(Received 9 September 1992; accepted 2 February 1993; Ms. 2275)